

Journal Pre-proof

Fixed magnetic nanoparticles: Obtaining anisotropy energy density from high field magnetization

D.G. Actis, I.J. Bruvera, G.A. Pasquevich, P. Mendoza Zélis

PII: S0304-8853(22)00847-2
DOI: <https://doi.org/10.1016/j.jmmm.2022.169962>
Reference: MAGMA 169962

To appear in: *Journal of Magnetism and Magnetic Materials*

Received date: 11 July 2022
Revised date: 31 August 2022
Accepted date: 11 September 2022

Please cite this article as: D.G. Actis, I.J. Bruvera, G.A. Pasquevich et al., Fixed magnetic nanoparticles: Obtaining anisotropy energy density from high field magnetization, *Journal of Magnetism and Magnetic Materials* (2022), doi: <https://doi.org/10.1016/j.jmmm.2022.169962>.

This is a PDF file of an article that has undergone enhancements after acceptance, such as the addition of a cover page and metadata, and formatting for readability, but it is not yet the definitive version of record. This version will undergo additional copyediting, typesetting and review before it is published in its final form, but we are providing this version to give early visibility of the article. Please note that, during the production process, errors may be discovered which could affect the content, and all legal disclaimers that apply to the journal pertain.

© 2022 Elsevier B.V. All rights reserved.



Fixed magnetic nanoparticles: obtaining anisotropy energy density from high field magnetization

D.G. Actis^a, I.J. Bruvera^a, G.A. Pasquevich^{a,b}, P. Mendoza Zélis^{a,b}

^a*Instituto de Física La Plata (IFLP-CONICET), Departamento de Física, Facultad de Ciencias Exactas, Universidad Nacional de La Plata (UNLP), La Plata, Argentina*

^b*Facultad de Ingeniería, Universidad Nacional de La Plata (UNLP), La Plata, Argentina*

Abstract

A simple method is proposed to obtain the effective anisotropy energy density K_{eff} of an assembly of randomly oriented magnetic nanoparticles, from their hysteresis loops. It involves the fitting of a high field asymptotic expression of the magnetization in inverse powers of the applied field H , up to H^{-3} . This is derived from the partition function formalism and the Stoner-Wohlfarth model for single domain nanoparticles. This method can be applied to ferrogels, frozen ferrofluids or magnetic nanoparticles powder (or any system where the nanoparticles are fixed in random directions, and not allowed to rotate), when dipolar interactions can be neglected. As a proof of concept, it is applied to a suspension of iron oxide nanoparticles in hexane, at different temperatures, obtaining the anisotropy energy density K_{eff} as a function of temperature below the fusion point.

Keywords: Magnetic nanoparticles, Anisotropy energy density, Fixed easy axes

1. Introduction

Magnetic nanoparticles (MNPs) are being extensively studied due to their multiple applications in technology[1], and in particular biomedicine[2, 3]. Single domain ferromagnetic MNPs present a well defined magnetic behaviour, where each particle is considered to have a permanent moment $\mu = M_S V$ and a preferential magnetization direction (easy axis). V is the particle's volume and M_S its saturation magnetization. In Stoner-Wohlfarth's

Email address: pmendoza@fisica.unlp.edu.ar (P. Mendoza Zélis)

Preprint submitted to Journal of Magnetism and Magnetic Materials August 31, 2022

8 model (SW)[4] the energy of such a particle in the presence of a magnetic field
 9 is the sum of two terms regarding the orientation of the particle's magnetic
 10 moment: the Zeeman energy for its tendency to align with the field, and
 11 the anisotropy energy for its tendency to align with the easy axis. This last
 12 term is proportional to the effective anisotropy energy density K_{eff} , which
 13 eventually includes magnetocrystalline, strain, magnetostrictive and shape
 14 contributions[5].

15 Depending on the application, the MNPs could be present in a liquid
 16 suspension (called ferrofluid)[6], or they may be fixed in solid matrices (as
 17 is the case of ferrogels, powders, or frozen ferrofluid[7]). This fixation of the
 18 MNPs in the solid prevents their displacement and rotation, and modifies in
 19 turn the magnetic response[8].

20 For a ferrofluid (FF) the equilibrium magnetization M in the direction
 21 of the applied field \vec{H} depends on particle saturation magnetization M_S ,
 22 particle density n , particle magnetic moment μ , temperature T , and field's
 23 magnitude H . The application of the partition function formalism to an
 24 assembly of free-to-rotate MNPs in thermal equilibrium at temperature T
 25 returns the Langevin response: $M = n \mu L(\alpha H)$ [5]. The factor α is the
 26 quotient $\mu_0 \mu / k_B T$, with μ_0 the vacuum permeability and k_B the Boltzmann
 27 constant. This result is obtained assuming enough inter-particle distance
 28 to disregard dipolar interactions between the MNPs[9]. While K_{eff} doesn't
 29 affect the FF equilibrium magnetization, it plays a pivotal role in its dynamic
 30 response to a time dependent field, such as the fields employed in biomedical
 31 applications[10, 11].

32 In the case of a poly-sized sample, a weighted average determines the final
 33 response, where the size distribution parameters, fundamentally mean and
 34 standard deviation, enter into play. In 1978 Chantrell et al.[12] presented a
 35 method to extract these two parameters for MNPs in a ferrofluid. It consisted
 36 in writing the asymptotic expressions for the Langevin function at low field
 37 (LF) and high field (HF), for a poly-sized sample. Measuring the LF slope in
 38 M vs. H and the HF slope in M vs. $1/H$, they obtained standard deviation
 39 and median particle diameter for said distribution.

40 For MNPs in a solid matrix, or ferrosolid (FS), the equilibrium magnetiza-
 41 tion depends not only on the value of the K_{eff} but on the easy axis directions
 42 distribution as well[8]. This can also be analyzed with the partition func-
 43 tion formalism, in particular for the case of random distribution of easy axes
 44 (FSR), as that configuration could model a MNP assembly solidified in the

45 absence of both external field and dipolar interactions[13]. However, the ex-
 46 pression obtained for the FSR doesn't have an analytical solution, such as
 47 the Langevin function in the case of the FF.

48 Asymptotic behaviour for randomly oriented MNPs in the HF region has
 49 been previously studied as “the law of approach to saturation” by Kneller et
 50 al. in 1962[14], and expressions up to H^{-2} have been used to extract K_{eff} from
 51 different samples[15, 16, 17], while Elrefai et al.[18] developed an empirical
 52 expression as a linear combination of zero anisotropy and infinite anisotropy
 53 curves. In order to reach lower uncertainty over the values obtained for K_{eff} ,
 54 we were motivated to find HF magnetic behaviour in larger powers of $1/H$
 55 allowing us to fit a wider field region.

56 In this work we propose and test a HF asymptotic expression up to H^{-3}
 57 for a FSR. The system studied is an hexane suspension of MNPs, frozen in the
 58 absence of an applied field. From hysteresis loops, at different temperatures
 59 below the freezing point, we make a least-squares fit with the HF expression
 60 and extract K_{eff} values. The method also provides mean particle magnetic
 61 moment $\langle \mu \rangle$, which is compared with the result of fitting the HF expression
 62 used by Chantrell, which is linear in H^{-1} .

63 2. Model

64 The equilibrium magnetization for an assembly of non-interacting MNPs
 65 in an external field may be obtained employing the partition function for-
 66 malism [19, 20].

67 The MNPs' anisotropy is due to several contributions (magnetocrys-
 68 talline, stress, shape, etc.). We consider an effective uniaxial anisotropy
 69 energy density K_{eff} , and thus the energy of the individual particle can be
 70 written as:

$$E = -\mu_0 \mu H [\hat{u} \cdot \hat{h}] - \mu \frac{K_{\text{eff}}}{M_S} [\hat{a} \cdot \hat{u}]^2, \quad (1)$$

71 where μ/M_S is the particle's volume, and \hat{a} , \hat{h} and \hat{u} are the directions of the
 72 anisotropy easy axis, the applied field and the particle's magnetic moment,
 73 respectively. The temperature is taken into account in the partition function
 74 dividing the nanoparticle energy by $k_B T$, obtaining the reduced energy

$$\epsilon = \frac{E}{k_B T} = -\rho [\hat{u} \cdot \hat{h}] - \lambda [\hat{a} \cdot \hat{u}]^2, \quad (2)$$

75 where $\rho = \mu\mu_0 H/k_B T$ and $\lambda = \mu K_{\text{eff}}/M_S k_B T$ are dimensionless parameters, the quotient of Zeeman energy and thermal energy and the quotient of
 76 anisotropy energy and thermal energy, respectively.
 77

78 The form of the partition function is different if we consider free-to-rotate
 79 nanoparticles or a solid matrix with fixed MNPs. We present both treatments
 80 separately.

81 2.1. Ferrofluid

82 In this case, the MNPs' easy axis directions are degrees of freedom, so we
 83 have the partition function

$$z_{\text{FF}}(N, \rho, \lambda) = \left[\iint e^{-\epsilon(\rho, \lambda, \Omega_a, \Omega_u)} d\Omega_a d\Omega_u \right]^N, \quad (3)$$

84 where N is the number of particles, Ω_a the easy axes solid angle, and Ω_u the
 85 magnetic moment solid angle. The projection of the magnetization in the
 86 applied field's direction is calculated as

$$M_{\text{FF}} = n \mu \langle \hat{u} \cdot \hat{h} \rangle = \frac{n \mu}{N} \frac{\partial}{\partial \rho} \log(z_{\text{FF}}), \quad (4)$$

87 where n is the particle density. The result is the well known Langevin
 88 response[20]:

$$M_{\text{FF}} = n \mu \left(\coth(\rho) - \frac{1}{\rho} \right) = n \mu L(\rho) \quad (5)$$

89 This magnetization is independent of the value of λ , that is to say independent
 90 of K_{eff} .

91 If the MNPs have a size distribution (and therefore a magnetic moment
 92 distribution), this can be incorporated to the theoretical magnetic response.
 93 We construct a linear superposition of eq. 5 expressing ρ in terms of μ ,
 94 obtaining the following response for poly-sized systems:

$$M_{\text{FF}}^P(H) = n \int_0^{\infty} \mu f(\mu) L\left(\frac{\mu_0 H \mu}{k_B T}\right) d\mu. \quad (6)$$

95 where $f(\mu)d\mu$ represents the fraction of particles with magnetic moment be-
 96 tween μ and $\mu + d\mu$. For fine particle systems the LogNormal distribution
 97 is usually encountered[21]. The resulting M_{FF}^P may be fitted to a M vs. H

98 curve as a whole, with the method of least-squares, obtaining distribution
99 parameters and n for a given T .

100 Chantrell et al.[12] proposed a method to obtain the size distribution's
101 mean value and standard deviation directly from simple asymptotic expres-
102 sions. For the FF we have the LF and HF responses of the mono-sized
103 Langevin function:

$$\text{LF} \quad \frac{M_{\text{FF}}(\rho)}{n\mu} = \frac{\rho}{3} + \mathcal{O}(\rho^3) \quad (7)$$

$$\text{HF} \quad \frac{M_{\text{FF}}(\rho)}{n\mu} = 1 - \frac{1}{\rho} + \mathcal{O}(e^{-2\rho}) \quad (8)$$

104 The corresponding poly-sized first orders can be given in terms of the
105 mean magnetic moment $\langle\mu\rangle$ and the mean square magnetic moment $\langle\mu^2\rangle$:

$$\text{LF} \quad M_{\text{FF}}^P(H) \approx n\langle\mu\rangle \frac{\mu_0 H \langle\mu^2\rangle}{3k_B T \langle\mu\rangle} = \frac{n\langle\mu^2\rangle}{3k_B T} \mu_0 H \quad (9)$$

$$\text{HF} \quad M_{\text{FF}}^P(H) \approx n\langle\mu\rangle \left(1 - \frac{k_B T}{\langle\mu\rangle \mu_0 H}\right) \quad (10)$$

106 It is concluded that the LF slope in M vs. H is proportional to $\langle\mu^2\rangle$, while
107 the the HF slope in M vs. $1/H$ is proportional to $1/\langle\mu\rangle$.

108 2.2. Ferrosolid

109 The FS has a corresponding partition function where the anisotropy di-
110 rections are not degrees of freedom but rather each nanoparticle has a fixed
111 easy axis direction \hat{a}_i , and consequently fixed angles Ω_{a_i} :

$$z_{\text{FS}}(N, \rho, \lambda, \Omega_{a_i}) = \prod_{i=0}^N \int e^{-\epsilon(\rho, \lambda, \Omega_{a_i}, \Omega_u)} d\Omega_u. \quad (11)$$

112 The integral expression for the sample magnetization takes the form

$$M_{\text{FS}} = \frac{n\mu}{N} \frac{\partial}{\partial \rho} \log(z_{\text{FS}}) \quad (12)$$

$$M_{\text{FS}}(\rho, \lambda) = n\mu \int \left[\frac{\int e^{-\epsilon(\rho, \lambda, \Omega_a, \Omega_u)} \hat{u} \cdot \hat{a} d\Omega_u}{\int e^{-\epsilon(\rho, \lambda, \Omega_a, \Omega_u)} d\Omega_u} \right] g(\Omega_a) d\Omega_a, \quad (13)$$

113 where $g(\Omega_a)$ is the easy axis directions distribution and the integral is taken
 114 over all possible directions. An analytic solution can't be found for the entire
 115 field range for an arbitrary distribution $g(\Omega_a)$. Yet asymptotic behaviours
 116 may be obtained: for LF expanding the integrals with Taylor series in powers
 117 of ρ at $\rho = 0$; and for HF expanding the integrands at Ω_u in the direction
 118 of the field (with Laplace's method, see for example [22]), and the result in
 119 powers of $1/\rho$.

120 In the appendix we write asymptotic expressions for arbitrary $g(\Omega_a)$, and
 121 compare the responses for specific configurations (all easy axes either parallel
 122 or perpendicular to the applied field) with previously known results.

123 For a FS with randomly oriented MNPs (FSR) we have a constant value
 124 for the distribution $g(\Omega_a) = 1/4\pi$. The resulting magnetization M_{FSR} is
 125 consistently lower than M_{FF} for a given value of ρ , and the difference between
 126 both moments increases with the value of λ [8]. The asymptotic expressions
 127 take the form

$$\text{LF} \quad \frac{M_{\text{FSR}}(\rho, \lambda)}{n\mu} = \frac{\rho}{3} + \mathcal{O}(\rho^3) \quad (14)$$

$$\text{HF} \quad \frac{M_{\text{FSR}}(\rho, \lambda)}{n\mu} = 1 - \frac{1}{\rho} - \frac{4}{15} \left(\frac{\lambda}{\rho}\right)^2 + \left(\frac{4}{3} - \frac{16\lambda}{105}\right) \frac{\lambda^2}{\rho^3} + \\ + \left(\frac{-12}{5} + \frac{32\lambda}{35}\right) \frac{\lambda^2}{\rho^4} + \mathcal{O}(\rho^{-5}) \quad (15)$$

Writing the first orders for poly-sized systems in terms of the applied field
 we obtain:

$$\text{LF} \quad M_{\text{FSR}}^P(H) \approx n \langle \mu \rangle \frac{\mu_0 H \langle \mu^2 \rangle}{3k_B T \langle \mu \rangle} = \frac{n \langle \mu^2 \rangle}{3k_B T} \mu_0 H \quad (16)$$

$$\text{HF} \quad M_{\text{FSR}}^P(H) \approx n \langle \mu \rangle \left(1 - \frac{k_B T}{\langle \mu \rangle \mu_0 H} - \frac{4}{15} \left(\frac{K_{\text{eff}}}{M_S}\right)^2 \frac{1}{(\mu_0 H)^2} + \right. \\ \left. + \left(\frac{4 k_B T}{3 \langle \mu \rangle} - \frac{16 K_{\text{eff}}}{105 M_S}\right) \left(\frac{K_{\text{eff}}}{M_S}\right)^2 \frac{1}{(\mu_0 H)^3} \right) \quad (17)$$

128 We have assumed that neither K_{eff} nor M_S are functions of the particle's
 129 size (and therefore, of its magnetic moment). Expressions up to H^{-2} have
 130 been previously employed to obtain K_{eff} [15, 16, 17]. We take into account

131 the next term, increasing the available field range for the fit while keeping
132 the same number of fitting parameters in the analysis.

133 We notice the coincidence of first order LF and HF responses between
134 FF and FSR (the HF response up to H^{-1} is the same for FS as well, see
135 appendix). This justifies using Chantrell's method even for FSR, at high
136 enough fields that the magnetic moment is accurately represented by the
137 first two HF terms. To explore this possibility we propose considering a field
138 range where the H^{-2} term is small in absolute value compared to the H^{-1}
139 term:

$$\frac{k_B T}{\langle \mu \rangle \mu_0 H} \gg \frac{4}{15} \left(\frac{K_{\text{eff}}}{M_S} \right)^2 \frac{1}{(\mu_0 H)^2} \quad (18)$$

$$\mu_0 H \gg \frac{4}{15} \left(\frac{K_{\text{eff}}}{M_S} \right)^2 \frac{\langle \mu \rangle}{k_B T} = \mu_0 H_1. \quad (19)$$

140 H_1 here serves as a reference field in terms of the system's parameters. To
141 apply Chantrell's method to a FSR we take care to work well above H_1 ;
142 that's the region where M is linear in $1/H$.

143 For our proposed method we take the terms from eq. 17 into account. We
144 need to explore lower fields than those used for Chantrell's method, allowing
145 us to extract K_{eff} from equilibrium magnetization measurements. For that we
146 consider a region where the H^{-4} term (the ρ^{-4} term in eq. 15) is neglectable.
147 Since the H^{-3} term might be zero depending on the value of λ , we measure
148 the H^{-4} term against the H^{-2} one. This leads to the condition:

$$\mu_0 H \gg \frac{k_B T}{\langle \mu \rangle} \sqrt{\left| 9 - \frac{24 K_{\text{eff}} \langle \mu \rangle}{7 M_S k_B T} \right|} = \mu_0 H_2, \quad (20)$$

149 where H_2 will serve as a reference field for our HF expression.

150 3. Materials and Methods

151 We study a sample, originally 50 μL of FF, iron oxide MNPs suspended
152 in hexane at a mass concentration of 3.4(3) g/L. TEM images were taken
153 in order to provide a reference for the size distribution of the particles, the
154 results indicating a narrow size distribution of spherical crystalline particles.
155 The TEM diameter distribution was fitted with a lognormal distribution,

156 obtaining a mean diameter of 9.5 nm and a standard deviation of 1.7 nm for
 157 the diameter (fig. 1). The inter-particle distance obtained from concentration
 158 and mean size indicates a separation of 110(20) nm, well over the 3 diameters
 159 limit established for dipolar interactions[23].

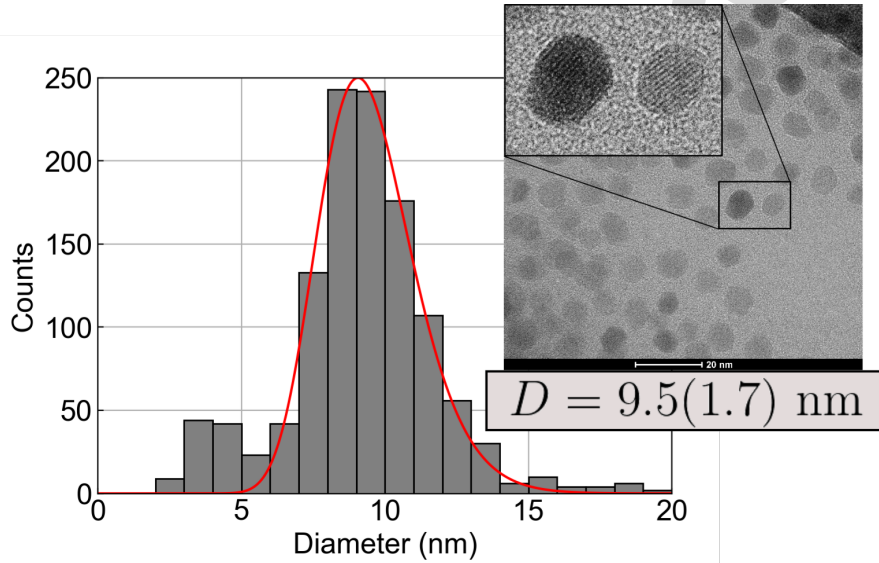


Figure 1: Size distribution from TEM images and corresponding fit. Inset: TEM image example with a magnification showing the crystallinity of the particles.

160 Hysteresis loops of the sample were obtained at different temperatures (5
 161 K, 10 K, 40 K, 160 K, and 220 K) using a superconducting quantum interference
 162 device (SQUID) magnetometer (Quantum Design, MPMS XL), see fig.
 163 2. The maximum applied field was 3600 kA/m, or 4.5 T for $B = \mu_0 H$. As
 164 hexane fusion temperature lies at 178 K, only the highest temperature (220
 165 K) corresponds to a FF, while all the others correspond to the frozen FSR.
 166 It has been reported that even at temperatures below the fusion tempera-
 167 ture the particles can rotate at a “premelting stage”, due to the presence
 168 of an interfacial liquid between MNPs and the frozen liquid[24, 25]. This
 169 premelting stage can be detected through zero-field-cooling and field-cooling
 170 experiments [25], which we have performed ensuring that at 160 K our parti-
 171 cles are prevented from both displacement and rotation. Also, we took care

172 to freeze the sample in the absence of applied field, in order to guarantee the
 173 random distribution of MNP easy axes.

174 At 40 K and below we observe coercivity, indicating that at least a frac-
 175 tion of the MNPs are in the blocked state, not reaching thermodynamic
 176 equilibrium at low fields[26]. We consider that above a certain irreversibility
 177 field $H_{\text{irr}}(T)$, every particle's energy profile has only one minimum, populated
 178 with Boltzmann statistics[27]. $H_{\text{irr}}(T)$ is determined as the field where both
 179 M branches coincide, and magnetization values measured above that field
 180 correspond to equilibrium.

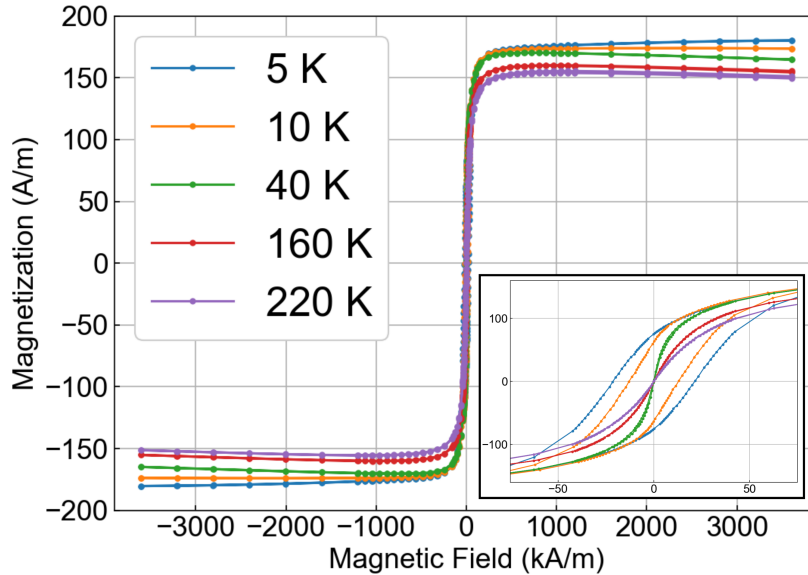


Figure 2: Magnetization (magnetic moment per unit sample volume) M vs. magnetic field H for the same sample of MNPs in hexane at different temperatures. Only the 220 K measurement is made above the fusion temperature of hexane. Inset: magnification of the coercivity region.

181 4. Discussion

182 At first, the full Langevin response for a poly-sized system (eq. 6), plus a
 183 diamagnetic contribution, was fitted to the FF at 220 K, assuming a LogNor-

184 mal distribution for the MNPs. From this fit, applied using the totality of the
 185 loop, we obtained values for the sample's particle density $n = 1.23(1) \times 10^{21}$
 186 m^{-3} , and the mean magnetic moment at 220 K: $\langle \mu \rangle = 1.40(1) \times 10^4 \mu_B$.
 187 While $\langle \mu \rangle$ is expected to vary with temperature according to Bloch's law[5],
 188 the value of n remains the same for all temperatures. For FSR analysis we
 189 fix n in this value to reduce the number of fitting parameters.

190 Matching the value of $\langle \mu \rangle$ from the fit with the TEM mean diameter
 191 ($\langle D \rangle = 9.55(8)$ nm) gives a particle saturation magnetization $M_S = 258(7)$
 192 kA/m, in accord with known values for iron oxide nanoparticles[28].

$T(\text{K})$	$H_c(\text{kA/m})$	$H_{\text{irr}}(\text{kA/m})$	$H_1(\text{kA/m})$	$H_2(\text{kA/m})$
5	21.29(3)	160(10)	1000	8
10	12.80(3)	160(10)	500	10
40	0.20(3)	30(10)	125	20
160	-	-	31	15

Table 1: Characteristic fields for the ferrosolid at each temperature. $H_1(H_2)$ represents the order of magnitude of lower fields where Chantrell's(our) HF expression is no longer valid

193 Then we proceeded to fit the asymptotic models to the FSR at different
 194 temperatures. We verified the presence of a region where the asymptotic ex-
 195 pressions are valid, evaluating H_1 (eq.19) and H_2 (eq.20), see table 1. Since
 196 the values for K_{eff} are taken from literature[29] at the specific temperature
 197 of 220 K, and we used M_S obtained also at that temperature, these fields are
 198 a gross estimation. In addition, the presence of coercivity at lower tempera-
 199 tures forced us to remain above the irreversibility field H_{irr} .

200 In table 2 we show values for mean magnetic moment $\langle \mu \rangle_{\text{Ch}}$, correspond-
 201 ing to fits of Chantrell's expression (eq. 10), made for fields above H_1 . The
 202 values for $\langle \mu \rangle$, M_S and K_{eff} were obtained fitting an expression up to H^{-3}
 203 (eq.17), well above H_2 , taking the same particle density n found for the FF.
 204 These fits are shown in fig. 3.

205 $K_{\text{eff}}(T)$ values obtained with our method are comparable with those found
 206 in the bibliography for iron oxide nanoparticles[28, 17]. Also there is a perfect
 207 agreement between the mean magnetic moments obtained with Chantrell's
 208 expression and ours. LF expressions are not applicable below the blocking
 209 temperature, but from the 160 K LF region we did obtain $\langle \mu^2 \rangle = 2.82(2)$
 210 μ_B^2 , which combined with the corresponding value of $\langle \mu \rangle$ gives a standard

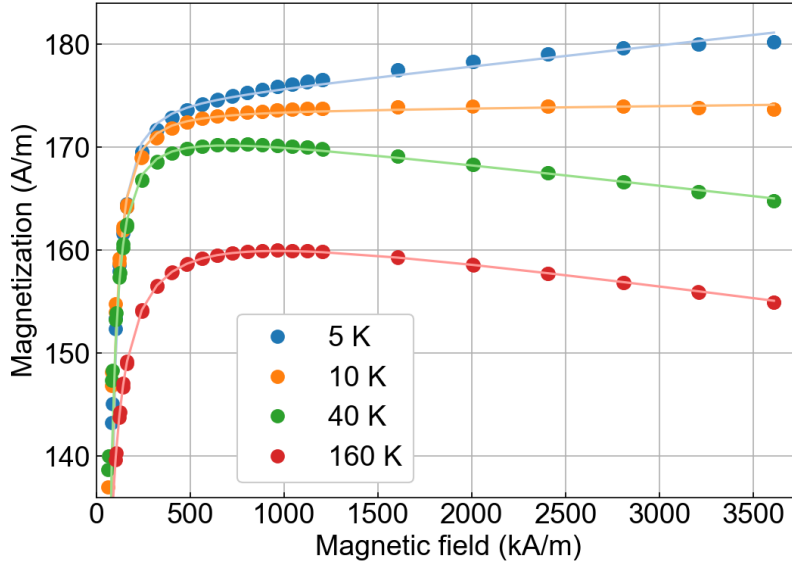


Figure 3: Data (points) and fit (continuous line) of eq.17 (up to H^{-3}) for the ferrosolid magnetization at different temperatures

$T(K)$	$\langle\mu\rangle_{Ch} (10^4\mu_B)$	$\langle\mu\rangle (10^4\mu_B)$	$M_S(kA/m)$	$K_{eff}(kJ/m^3)$
5	1.53(1)	1.52(1)	280(7)	21.3(6)
10	1.52(1)	1.51(1)	279(7)	20.1(6)
40	1.51(1)	1.51(1)	279(7)	18.7(5)
160	1.44(1)	1.44(1)	265(7)	12.2(4)

Table 2: Magnetic characteristics obtained from fitting the asymptotic expressions at the FS at different temperatures. The second column corresponds to fits of Chantrell's expression, while the others correspond to ours (up to H^{-3})

211 deviation of $8.6(2) \times 10^3 \mu_B$ for the particle magnetic moment.

212 We must comment on the high field susceptibility χ_{HF} that remains after
 213 saturation of the MNPs. It presents a change in sign between 10 and 40 K.
 214 In order to explain this behaviour we propose a sum of a diamagnetic con-
 215 tribution χ_D , independent of temperature, and a paramagnetic contribution

216 $\chi_P = C/T$, following Curie's law. Fitting this sum to χ_{HF} vs. temperature
 217 yields a diamagnetic susceptibility $\chi_D = -8.2(2) \times 10^{-5}$ in accord with re-
 218 ported values for hexane[30], and a Curie constant $C = 6(1) \times 10^{-4}$ K. The
 219 observed paramagnetism might be explained by a spin-disordered layer at
 220 the particle surface as discussed by [31, 32].

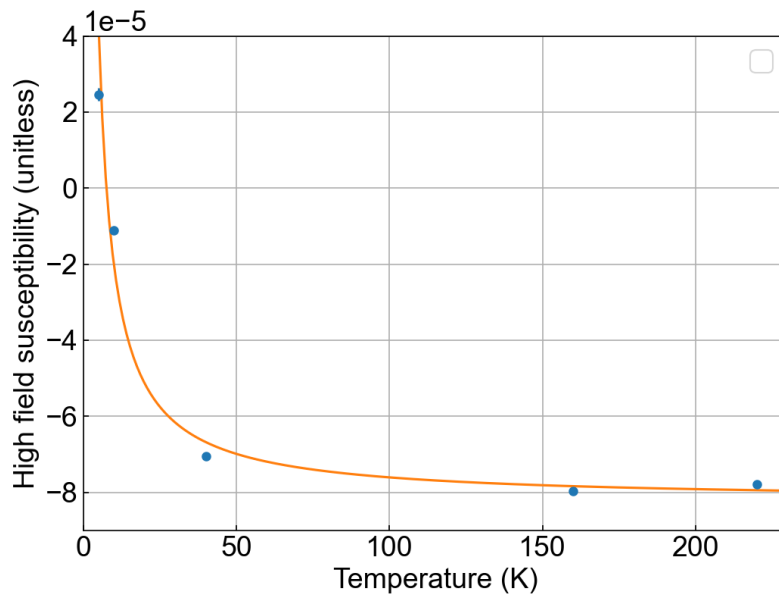


Figure 4: High field susceptibility vs. temperature, and fit of sum of paramagnetic ($\propto 1/T$) and diamagnetic (constant) contributions.

221 5. Conclusions

222 We have obtained an expression for the magnetic moment of a system
 223 of randomly oriented magnetic nanoparticles, in the high field region. This
 224 asymptotic expression in inverse powers of the applied field H , up to H^{-3} ,
 225 is derived from the partition function formalism and the Stoner-Wohlfarth
 226 model for single domain nanoparticles. The parameters involved are the par-
 227 ticle density n , mean particle magnetic moment $\langle\mu\rangle$, temperature T , particle
 228 saturation magnetization M_S and anisotropy energy density K_{eff} .

229 With this expression we have devised a simple method, choosing a suitable
 230 field region to apply least squares fits to the magnetic moment measurements,
 231 to obtain among other parameters the effective magnetic anisotropy. As
 232 a proof of concept, we have applied this method to an hexane suspension
 233 of randomly oriented iron oxide magnetic nanoparticles, obtaining K_{eff} for
 234 different temperatures below hexane's fusion point. Results are in the [12,22]
 235 kJ/m³ range, decreasing with temperature, compatible with known values for
 236 similar systems.

237 This method may be applied to ferrogels, frozen ferrofluids, or magnetic
 238 nanoparticles in dried powder, when the samples are prepared in the absence
 239 of field and dipolar interactions can be disregarded. With a magnetic moment
 240 measurement (such as those made with a VSM), at high enough fields, and
 241 knowing the particle's saturation magnetization M_S , the system's K_{eff} is
 242 obtained.

243 We have also shown that a simpler expression proposed by Chantrell et
 244 al. for a ferrofluid, up to H^{-1} , is valid for MNPs with randomly oriented
 245 easy axes as well, in determined field region. While K_{eff} cannot be obtained
 246 in this fashion, the same $\langle\mu\rangle$ is found with either method when both are
 247 simultaneously applicable.

248 Acknowledgements

249 This work has been partially supported by the National Research Council
 250 of Argentina (CONICET, grant 11220200102280CO), Universidad Nacional
 251 de La Plata (grant PID 11X897) and Agencia Nacional de Promoción
 252 Científica y Tecnológica (grant PICT 2017-1748). We thank Prof. Francisco
 253 H. Sanchez for the fruitful discussions that enriched this work.

254 Appendix

For the particular case when all easy axes are parallel to the applied field,
 eq. 13 has an analytic solution in terms of the imaginary error function:

$$\frac{M_{\text{par}}(\rho, \lambda)}{n\mu} = \frac{2 e^{\lambda + \frac{\rho^2}{4\lambda}} \sinh(\rho)}{\sqrt{\pi\lambda} \left(\operatorname{erfi}\left(\frac{\rho+2\lambda}{2\sqrt{\lambda}}\right) - \operatorname{erfi}\left(\frac{\rho-2\lambda}{2\sqrt{\lambda}}\right) \right)} - \frac{\rho}{2\lambda} \quad (.1)$$

255 This response lies between two extremes: its lower bound is the Langevin
 256 function $L(\rho)$ in the $\lambda \rightarrow 0$ limit, and its higher bound is the hyperbolic

257 tangent $\tanh(\rho)$ in the $\lambda \rightarrow \infty$ limit. The hyperbolic tangent is the result of
 258 the two level model for the particle moment[8].

259 For a more general case we have found asymptotic expressions for equation
 260 13, for arbitrary easy axis directions distribution $g(\Omega_a)$, that were left out of
 261 the main body of this work. These are

$$\text{LF} \quad \frac{M_{\text{FS}}(\rho, \lambda)}{n\mu} = \rho \left(\frac{1}{3} + \left(\frac{e^\lambda}{\sqrt{\pi\lambda} \operatorname{erfi}(\sqrt{\lambda})} - \frac{1}{2\lambda} - \frac{1}{3} \right) \langle P_2(\hat{h} \cdot \hat{a}) \rangle \right) + \quad (.2)$$

$$+ \mathcal{O}(\rho^3) \quad (.3)$$

$$\text{HF} \quad \frac{M_{\text{FS}}(\rho, \lambda)}{n\mu} = 1 - \frac{1}{\rho} - \frac{4}{15} \frac{\lambda^2}{\rho^2} + \frac{2}{\rho^2} \left[\lambda \langle P_2(\hat{h} \cdot \hat{a}) \rangle + \right. \\ \left. + \frac{2\lambda^2}{7} \left(\frac{4}{5} \langle P_4(\hat{h} \cdot \hat{a}) \rangle - \frac{1}{3} \langle P_2(\hat{h} \cdot \hat{a}) \rangle \right) \right] + \mathcal{O}(\rho^{-3}) \quad (.4)$$

262 where P_2 and P_4 are the Legendre polynomials of second and fourth order,
 263 respectively, and the averages $\langle \rangle$ are taken over the distribution of angles
 264 between the easy axis and the applied field. For example

$$\langle P_2(\hat{h} \cdot \hat{a}) \rangle = \int P_2(\hat{h} \cdot \hat{a}) g(\Omega_a) d\Omega_a \quad (.5)$$

265 If we consider the particular case where all easy axes are parallel to the
 266 applied field the resulting expressions are much simplified, as $P_n(1) = 1$:

$$\text{LF} \quad \frac{M_{\text{par}}(\rho, \lambda)}{n\mu} = \rho \left(\frac{e^\lambda}{\sqrt{\pi\lambda} \operatorname{erfi}(\sqrt{\lambda})} - \frac{1}{2\lambda} \right) + \mathcal{O}(\rho^3) \quad (.6)$$

$$\text{HF} \quad \frac{M_{\text{par}}(\rho, \lambda)}{n\mu} = 1 - \frac{1}{\rho} + \left(1 - \frac{\lambda}{15} \right) \frac{2\lambda}{\rho^2} + \mathcal{O}(\rho^{-3}) \quad (.7)$$

267 These are the asymptotic expressions of eq. .1. The LF response is equal to
 268 the one found by Yasumori in terms of infinite sums[20].

269 For easy axes perpendicular to the applied field, we have $P_2(0) = -1/2$,
 270 $P_4(0) = 3/8$, so

$$\text{LF} \quad \frac{M_{\text{per}}(\rho, \lambda)}{n \mu} = \frac{\rho}{2} \left(1 - \frac{e^\lambda}{\sqrt{\pi \lambda} \operatorname{erfi}(\sqrt{\lambda})} + \frac{1}{2\lambda} \right) + \mathcal{O}(\rho^3) \quad (.8)$$

$$\text{HF} \quad \frac{M_{\text{per}}(\rho, \lambda)}{m_S} = 1 - \frac{1}{\rho} - \frac{\lambda}{\rho^2} + \mathcal{O}(\rho^{-3}) \quad (.9)$$

271 Once again we find agreement with expressions obtained by Yasumori for HF
272 behaviour, and for LF in the limit $\lambda \ll 1$.

273 References

- 274 [1] M. Naito, T. Yokoyama, K. Hosokawa, K. Nogi, Nanoparticle technology
275 handbook, Elsevier, 2018.
- 276 [2] Q. Pankhurst, N. Thanh, S. Jones, J. Dobson, Progress in applications
277 of magnetic nanoparticles in biomedicine, *Journal of Physics D: Applied*
278 *Physics* 42 (2009) 224001.
- 279 [3] A. Neumann, K. Gräfe, A. von Gladiss, M. Ahlborg, A. Behrends,
280 X. Chen, J. Schumacher, Y. B. Soares, T. Friedrich, H. Wei, et al., Re-
281 cent developments in magnetic particle imaging, *Journal of Magnetism*
282 *and Magnetic Materials* 550 (2022) 169037.
- 283 [4] E. C. Stoner, E. Wohlfarth, A mechanism of magnetic hysteresis in
284 heterogeneous alloys, *Philosophical Transactions of the Royal Society*
285 *of London. Series A, Mathematical and Physical Sciences* 240 (1948)
286 599–642.
- 287 [5] B. D. Cullity, C. D. Graham, Introduction to magnetic materials, John
288 Wiley & Sons, 2011.
- 289 [6] M. Kole, S. Khandekar, Engineering applications of ferrofluids: A re-
290 view, *Journal of Magnetism and Magnetic Materials* 537 (2021) 168222.
- 291 [7] R. J. Tackett, J. Thakur, N. Mosher, E. Perkins-Harbin, R. E. Kumon,
292 L. Wang, C. Rablau, P. P. Vaishnava, A method for measuring the néel
293 relaxation time in a frozen ferrofluid, *Journal of Applied Physics* 118
294 (2015) 064701.

- 295 [8] J. Carrey, B. Mehdaoui, M. Respaud, Simple models for dynamic hys-
296 teresis loop calculations of magnetic single-domain nanoparticles: Ap-
297 plication to magnetic hyperthermia optimization, *Journal of applied*
298 *physics* 109 (2011) 083921.
- 299 [9] M. Woińska, J. Szczytko, A. Majhofer, J. Gosk, K. Dziatkowski,
300 A. Twardowski, Magnetic interactions in an ensemble of cubic nanopar-
301 ticles: A monte carlo study, *Physical Review B* 88 (2013) 144421.
- 302 [10] A. B. Salunkhe, V. M. Khot, S. Pawar, Magnetic hyperthermia with
303 magnetic nanoparticles: a status review, *Current topics in medicinal*
304 *chemistry* 14 (2014) 572–594.
- 305 [11] K. M. Krishnan, Biomedical nanomagnetism: a spin through possibilities
306 in imaging, diagnostics, and therapy, *IEEE transactions on magnetics*
307 46 (2010) 2523–2558.
- 308 [12] R. Chantrell, J. Popplewell, S. Charles, Measurements of particle size
309 distribution parameters in ferrofluids, *IEEE Transactions on Magnetism*
310 14 (1978) 975.
- 311 [13] D. Clarke, C. Marquina, D. Lloyd, G. Vallejo-Fernandez, Effect of
312 the distribution of anisotropy constants on the magnetic properties of
313 iron oxide nanoparticles, *Journal of Magnetism and Magnetic Materials*
314 (2022) 169543.
- 315 [14] E. Kneller, A. Seeger, H. Kronmüller, *Ferromagnetismus*, Springer, 1962.
- 316 [15] G. Hadjipanayis, D. J. Sellmyer, B. Brandt, Rare-earth-rich metallic
317 glasses. i. magnetic hysteresis, *Physical Review B* 23 (1981) 3349.
- 318 [16] I. Abu-Aljarayesh, A. Al-Bayrakdar, S. H. Mahmood, The effect of
319 heating on the magnetic properties of Fe_3O_4 fine particles, *Journal of*
320 *Magnetism and Magnetic Materials* 123 (1993) 267–272.
- 321 [17] L. H. Nguyen, V. T. K. Oanh, P. H. Nam, D. H. Doan, N. X. Truong,
322 N. X. Ca, P. T. Phong, L. V. Hong, T. D. Lam, Increase of magnetic
323 hyperthermia efficiency due to optimal size of particles: theoretical and
324 experimental results, *Journal of Nanoparticle Research* 22 (2020).

- 325 [18] A. L. Elrefai, T. Sasayama, T. Yoshida, K. Enpuku, Empirical expres-
326 sion for dc magnetization curve of immobilized magnetic nanoparticles
327 for use in biomedical applications, *AIP Advances* 8 (2017) 056803.
- 328 [19] F. West, General superparamagnetic behavior of an aligned assembly
329 of uniaxially anisotropic particles, *Journal of Applied Physics* 32 (1961)
330 S249.
- 331 [20] I. Yasumori, D. Reinen, P. Selwood, Anisotropic behavior in superpara-
332 magnetic systems, *Journal of Applied Physics* 34 (1963) 3544.
- 333 [21] C. G. Granqvist, R. A. Buhrman, Ultrafine metal particles, *Journal of*
334 *Applied Physics* 47 (1976) 2200.
- 335 [22] R. Wong, *Asymptotic approximations of integrals*, SIAM, 2001.
- 336 [23] F. H. Sánchez, P. M. Zélis, M. Arciniegas, G. A. Pasquevich, M. F.
337 Van Raap, Dipolar interaction and demagnetizing effects in magnetic
338 nanoparticle dispersions: Introducing the mean-field interacting super-
339 paramagnet model, *Physical Review B* 95 (2017) 134421.
- 340 [24] M. Klokkenburg, B. H. Erne, A. P. Philipse, Thermal motion of magnetic
341 iron nanoparticles in a frozen solvent, *Langmuir* 21 (2005) 1187–1191.
- 342 [25] T. Wen, W. Liang, K. M. Krishnan, Coupling of blocking and melting
343 in cobalt ferrofluids, *Journal of Applied Physics* 107 (2010) 09B501.
- 344 [26] I. Bruvera, P. Mendoza Zélis, M. Pilar Calatayud, G. F. Goya, F. H.
345 Sánchez, Determination of the blocking temperature of magnetic
346 nanoparticles: The good, the bad, and the ugly, *Journal of Applied*
347 *Physics* 118 (2015) 184304.
- 348 [27] S. Mørup, C. Frandsen, M. F. Hansen, Uniform excitations in magnetic
349 nanoparticles, *Beilstein journal of nanotechnology* 1 (2010) 48–54.
- 350 [28] J. M. Orozco-Henao, D. F. Coral, D. Muraca, O. Moscoso-Londoño,
351 P. M. Zelis, M. B. F. van Raap, S. K. Sharma, K. R. Pirota, M. Knobel,
352 Effects of nanostructure and dipolar interactions on magnetohyperther-
353 mia in iron oxide nanoparticles, *The Journal of Physical Chemistry C*
354 120 (2016) 12796 – 12809.

- 355 [29] Z. Kakol, J. Sabol, J. M. Honig, Magnetic anisotropy of titanomagnetites
356 $\text{Fe}_{3-x}\text{Ti}_x\text{O}_4$, $0 \leq x \leq 0.55$, Physical Review B 44 (1991) 2198.
- 357 [30] S. R. Rao, G. Sivaramakrishnan, Diamagnetism of liquid mixtures,
358 Nature 128 (1931) 872–872.
- 359 [31] Z. Shaterabadi, G. Nabiyouni, G. F. Goya, M. Soleymani, The ef-
360 fect of the magnetically dead layer on the magnetization and the mag-
361 netic anisotropy of the dextran-coated magnetite nanoparticles, Applied
362 Physics A 128 (2022) 1–10.
- 363 [32] X. Batlle, A. Labarta, Finite-size effects in fine particles: magnetic and
364 transport properties, Journal of Physics D: Applied Physics 35 (2002)
365 R15.

-A method to obtain the effective anisotropy energy density of randomly oriented magnetic nanoparticles is proposed.

-This method can be applied to any system where the nanoparticles are fixed and not allowed to rotate.

-The method involves the fitting of a high field asymptotic expression of the magnetization.

-It is applied to a suspension of iron oxide nanoparticles in hexane to obtain K as a function of temperature, below the fusion point.

Declaration of interests

The authors declare that they have no known competing financial interests or personal relationships that could have appeared to influence the work reported in this paper.

The authors declare the following financial interests/personal relationships which may be considered as potential competing interests:

Journal Pre-proof